



## **ENGO 423: Geodesy**

Winter Term 2024

### **Lab Assignment 5: Local Geoid Modelling and Height Systems**

**Course Instructor:** Elena Rangelova

**Teaching Assistant:** Mohammad Javad Dehghan

**Date Submitted:** April 9<sup>th</sup> 2024

**Students:** Dylan Conley, 30140483  
Tavish Comrie, 30144899

#### **Academic Integrity Statement:**

We, Tavish Comrie, and Dylan Conley, certify that this is our own work, which has been done expressly for this course, either without the assistance of any other party or where appropriate, we have acknowledged the work of others. Further, we have read and understood the section in the university calendar on plagiarism/cheating/other academic misconduct, and we are aware of the implications thereof.

A handwritten signature in black ink, appearing to be 'DC' or similar initials.

A handwritten signature in black ink, appearing to be 'TC' or similar initials.

## Table of Contents

Introduction.....	1
Methodology and Results .....	1
Task 1.....	1
Task 1.1.....	1
Task 1.2.....	<b>Error! Bookmark not defined.</b>
Task 2.....	7
Task 2.1.....	<b>Error! Bookmark not defined.</b>
Task 2.2.....	<b>Error! Bookmark not defined.</b>
Task 3.....	<b>Error! Bookmark not defined.</b>
Task 3.1.....	<b>Error! Bookmark not defined.</b>
Task 3.2.....	<b>Error! Bookmark not defined.</b>
Task 3.3.....	<b>Error! Bookmark not defined.</b>
Conclusion .....	13
References.....	14
Appendix A: MATLAB Code .....	15

## List of Tables and Figures

Table 1: GRS80 Parameters Used in Calculations.....	<b>Error! Bookmark not defined.</b>
Figure 1: Geoid Height on Surface Degree Max =20.....	<b>Error! Bookmark not defined.</b>
Figure 2: Geoid Height on Surface, Degree Max =70 .....	<b>Error! Bookmark not defined.</b>
Figure 3: Geoid Height 375km Above Surface, Degree Max = 20.....	4
Figure 4: Geoid Height 375km Above Surface, Degree Max =70 .....	<b>Error! Bookmark not defined.</b>
Figure 5: Gravity Anomaly Degree Max =20 .....	<b>Error! Bookmark not defined.</b>

## Introduction

This lab was split into two sections. First, given normal heights and gravity values for multiple benchmarks, the Helmert and dynamic heights were computed along with the gravity anomalies and Bouguer gravity anomalies. Secondly, the remove-restore was used to determine the local geoid. Two executable files were, and short wavelengths and the long wavelengths were provided where they were then to be added together to calculate the high-resolution geoid in Alberta.

## Methodology and Results

### Task 1

#### Task 1.1

The first goal of this lab was to compute the Helmert and dynamic heights based on a set of normal heights ( $H^*$ ) and gravity values ( $g$ ) given at an assortment of benchmarks given in the Lab Handout [1]. To begin the geopotential numbers  $C$  were calculated at each benchmark using the following equation: [2]

$$(H^*)(\bar{\gamma}) = C$$

However, the mean ellipsoidal gravity value ( $\bar{\gamma}$ ) must first be computed using the following equation:

$$(\bar{\gamma}) = \gamma \left[ 1 - (2 + f + m - 2f \sin^2 \varphi) \frac{H^*}{a} + \left( \frac{H^*}{a} \right)^2 \right]$$

In which each ellipsoidal gravity value ( $\gamma$ ), is calculated using latitude with the Somigliana-Pizzetti formula shown below [3]:

$$\gamma = \gamma_a \frac{(1 + k \sin^2 \varphi)}{\sqrt{1 - e^2 \sin^2 \varphi}}$$

This equation uses  $\gamma_a$ ,  $k$ , and  $e$  which are given in the GRS-80 Handout [4].

Once the geopotential numbers were calculated for each benchmark, the Helmert/Orthometric height ( $H$ ) could be calculated. This process involved using the following formula to compute for  $H$ : [2]

$$H = \frac{C}{\bar{g}}$$

In which each mean gravity value needed to be iteratively calculated using the following equation: [2]

$$\bar{g} = g \pm 0.0424H$$

The process was iterative because the mean gravity is dependent on the orthometric height and vice-versa. Therefore, the first iteration involved the use of the normal height instead of the orthometric height to find a mean gravity. Once the first mean gravity was found, an Orthometric height could be calculated and then the process was repeated. This went on until the previous and current Orthometric heights calculated were within 1 mm of each other and the process was deemed to be successfully complete for the desired precision.

Once the Orthometric height was found, the difference between the Orthometric height and the normal height ( $H^* - H$ ) were found and plotted as a function of the normal height. This resulted in the following correlation table and plot:

Table 1: Correlation Matrix between Helmert and Normal Height Difference, and Normal Height

1	0.9768
0.9768	1

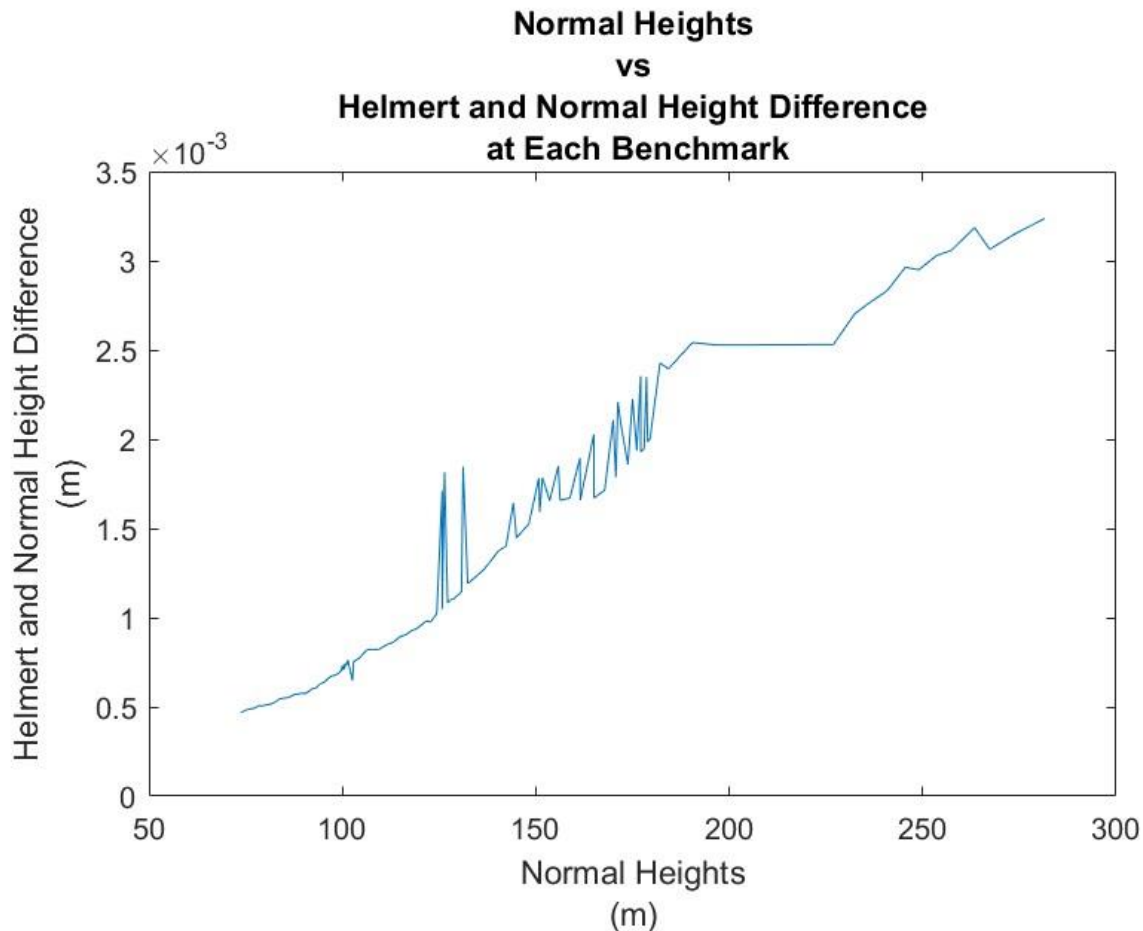


Figure 1: Helmert Vs Normal Height as function of Normal Height

Visible in Figure 1 and Table 1 there is a clear positive correlation between the normal and Helmert height differences and the normal heights themselves. As the Normal height increases, the difference increases as well in nearly a linear fashion visible both through a visual analysis of the plot and with the correlation of 0.9768 being very nearly 1 between the two axis. The linear relationship can be seen in that the Helmert and Normal Height difference is the geoid undulation. It looks at the distance between the geoid and the ellipsoid so it makes logical sense that as the normal height increases, the geoid undulation also increases.

Next, the geopotential numbers were used to compute the dynamic height ( $H^D$ ) at the given benchmarks using the normal gravity at a latitude of  $45^\circ$  on the ellipsoid. To first calculate the dynamic height, the

Somigliana-Pizzetti formula was used again to find the gravity at a latitude of  $45^\circ$ . This gravity value was found to be  $9.8061992 \text{ m/s}^2$  and was used in the following equation to find the dynamic height: [2]

$$H^D = \frac{C}{\gamma_{45^\circ}}$$

Where C was the geopotential number found at each benchmark.

The difference between the dynamic height and the Orthometric height was then plotted as a function with respect to the orthometric heights resulting in the following correlation matrix and plot:

Table 2: Correlation Matrix of the Difference Between the Helmert and Dynamic Height, and the Helmert Height

1	0.9985
0.9985	1

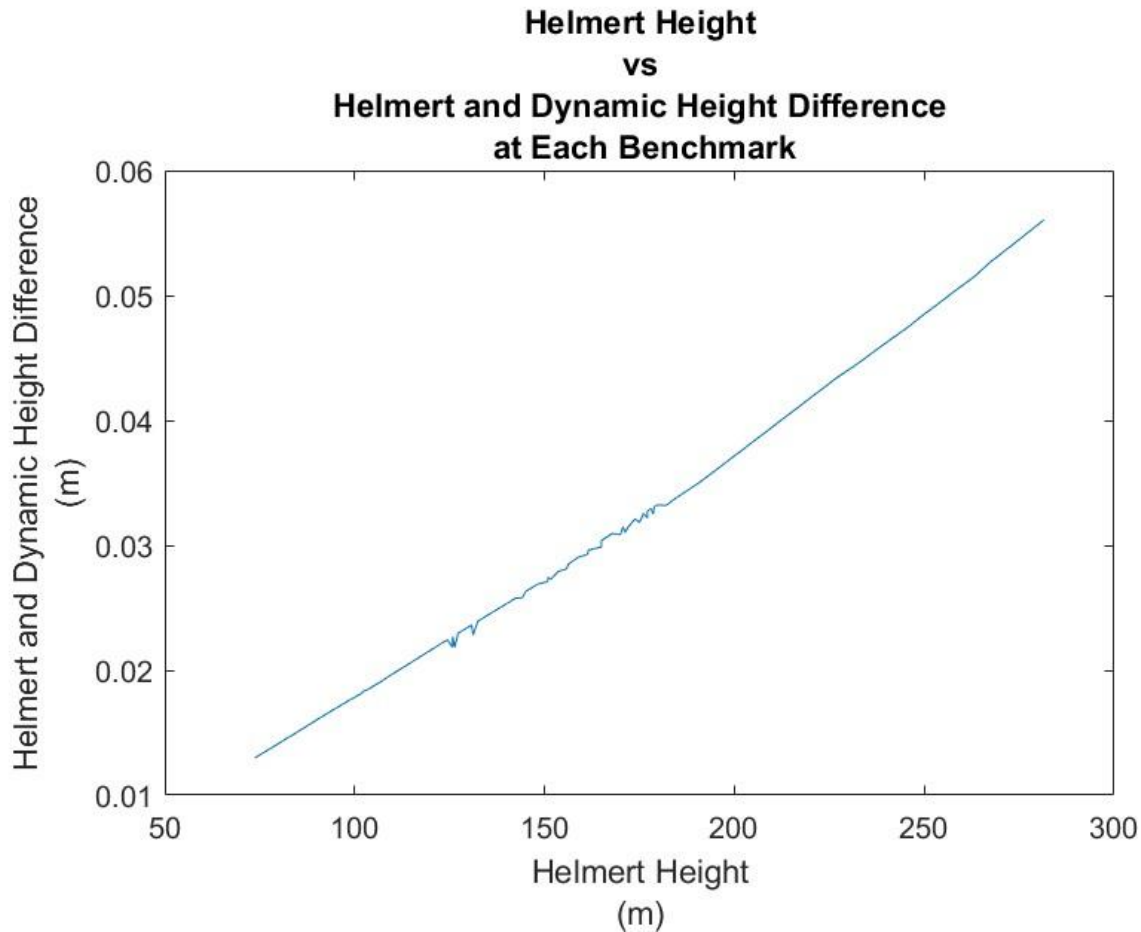


Figure 2: Helmert and Dynamic Height Difference vs Helmert Height

Figure 2 and Table 2 show a distinct positive linear correlation between the Helmert and Dynamic height difference with Helmert height itself. The differences are larger than the ones between the Helmert height and normal height however are still no greater than 6 centimeters. Because of how nearly perfectly linear the correlation is, it could be possible to model the differences and correct for it instead

of needing to calculate the dynamic heights themselves, while maintain a high precision. There are only a few visible disturbances from the linear trend however they are very small and eventually Figure 2 returns to showing a straight line once the Helmert height is over approximately 190 meters. This shows that the Helmert height is overall very linearly related to the ellipsoid as the dynamic height is based primarily on the ellipsoid. This is again very similar to the previous example in that the Helmert and dynamic height difference is very similar to the geoid undulation which increases as the Helmert height increases.

#### Task 1.2

First, the gravity anomalies were calculated at each benchmark and plotted as a function of the normal height. This was done using the following equation: [2]

$$\Delta g = g - \gamma(H^*)$$

Where: [2]

$$\gamma(H^*) = \gamma \left[ 1 - \frac{2}{a} (1 + f + m - 2f \sin^2 \varphi) H^* + 3 \frac{\gamma_a}{a^2} H^{*2} \right]$$

Using these equations, the gravity anomaly at each benchmark was calculated. The following table and plot reflect the results of these calculations:

*Table 3: Correlation Matrix between Gravity Anomaly and Normal Height*

1	0.9834
0.9834	1

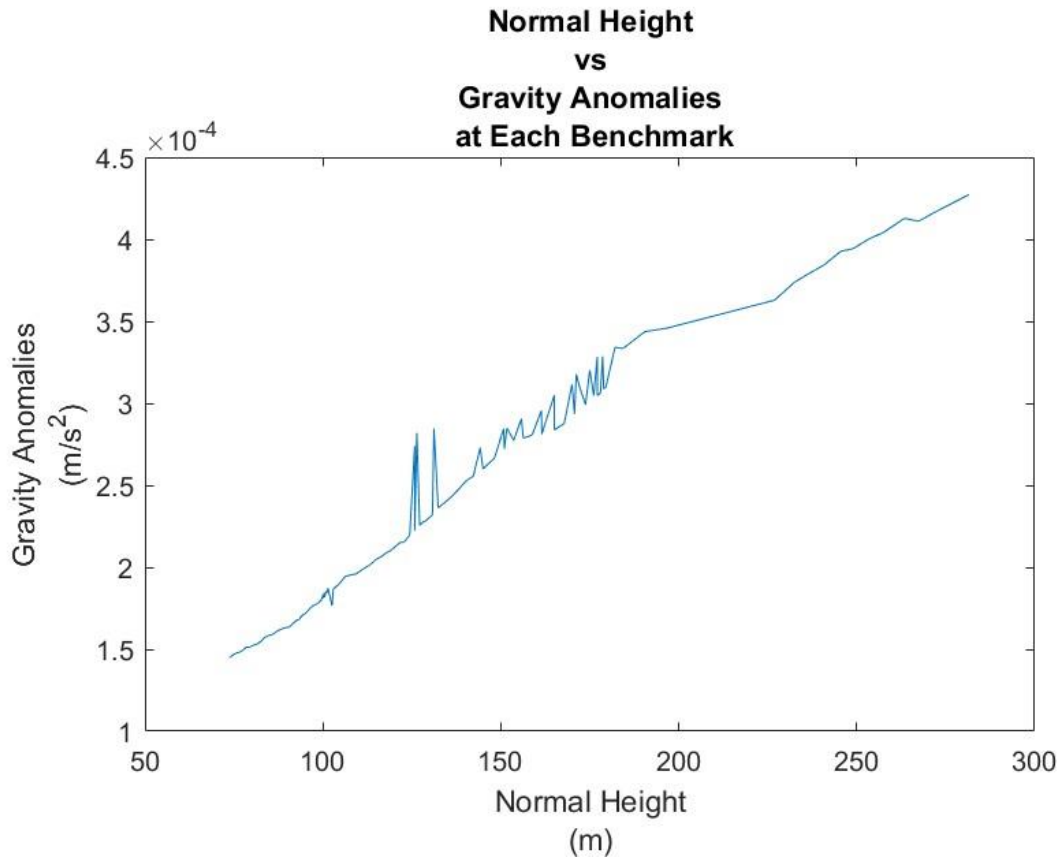


Figure 3: Gravity Anomalies Plotted Against Normal Height

Figure 3 and Table 3 are similar to the results found in Task 1.1 with a very high correlation being found between the gravity anomalies and the normal height. There are again visible changes from a linear path mostly between a normal height of 130 to 190 meters similar to Figures 1 and 2. The semi linear relationship can be understood by the formula for the gravity anomaly. It is in part related to the gravity values which is less correlated with the normal height and in part related to the ellipsoid gravity which is related to the normal height meaning ½ of the terms of the gravity anomaly are highly correlated with the normal height.

Next, the Bouguer anomalies were calculated very similarly to the gravity anomalies only adding one other term creating the following equation: [2]

$$\Delta g^B = g - \gamma(H^*) - 0.1119H^*$$

Once the Bouguer anomaly was found at each benchmark the following correlation matrix and graph were created:

Table 4: Correlation Matrix between Bouguer Anomaly and Normal Height

1	0.7985
0.7985	1

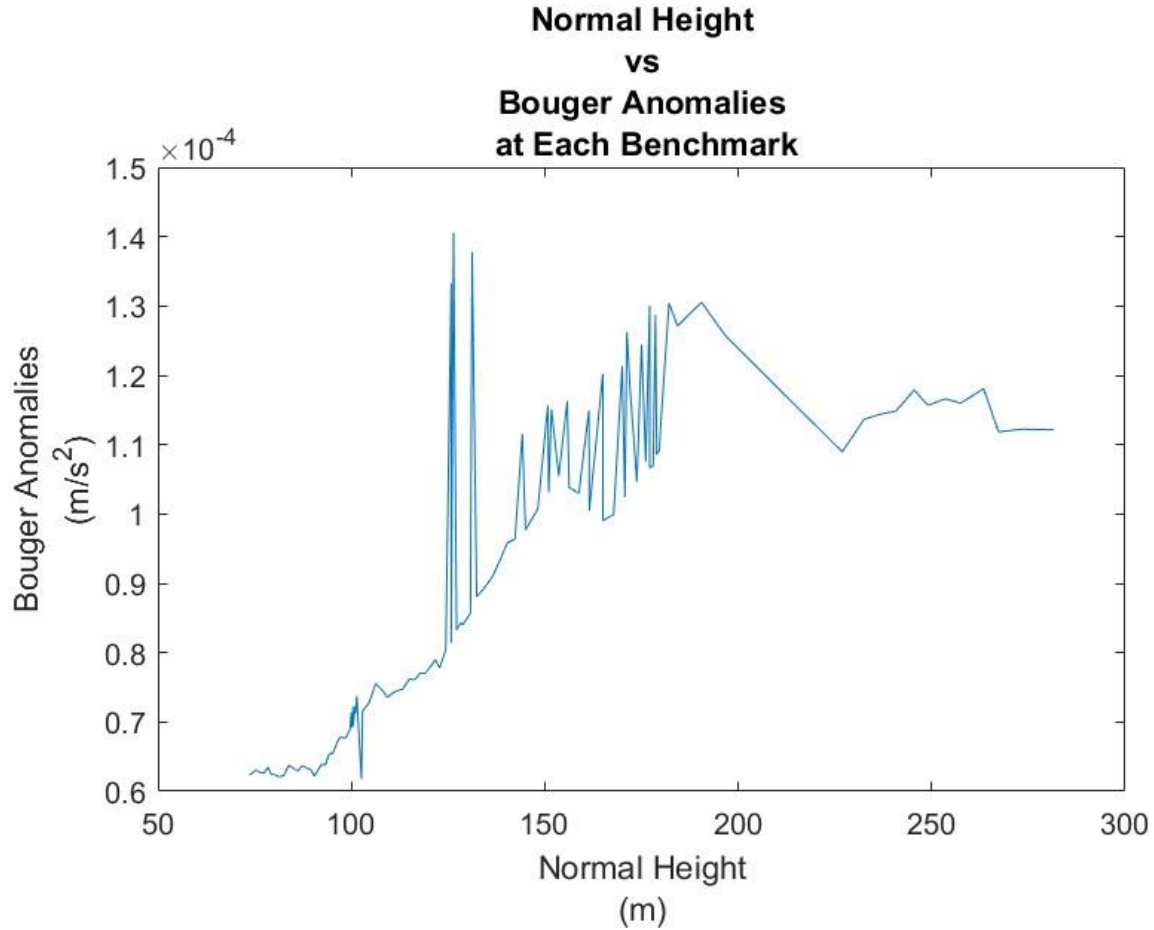


Figure 4: Bouguer Anomaly Plotted Against the Normal Height

Figure 4 and Table 4 differ from the previous results with a much less linear correlation value of only 0.7985. From a visual analysis of Figure 4, there are clearly much greater randomness to the values with some anomalies randomly increasing at specific benchmarks before returning back to what could potentially be expected. Furthermore, as the normal heights get larger, there is not the same continuance in the Bouguer anomalies as they nearly flatten out at a normal height of approximately 240 meters with no obvious correlation visible. The calculated correlation of 0.80 makes sense in that some of the terms for the bouguer anomaly are directly correlated with the normal height but not all of them are.

Finally, the Bouguer anomalies were used to estimate the difference between the normal height and the orthometric height. This was possible due to the following identity relating the difference to the Bouguer anomaly: [2]

$$(H^* - H)^B \approx \Delta g^B \frac{H}{\bar{\gamma}}$$

These difference values were then compared to the calculated difference found in Task 1.1 using a plot created in MATLAB and a correlation matrix between the two types of differences shown below:



Table 5: Correlation Matrix between Bouguer Anomaly Difference and Orthometric Height

1	0.949
0.949	1

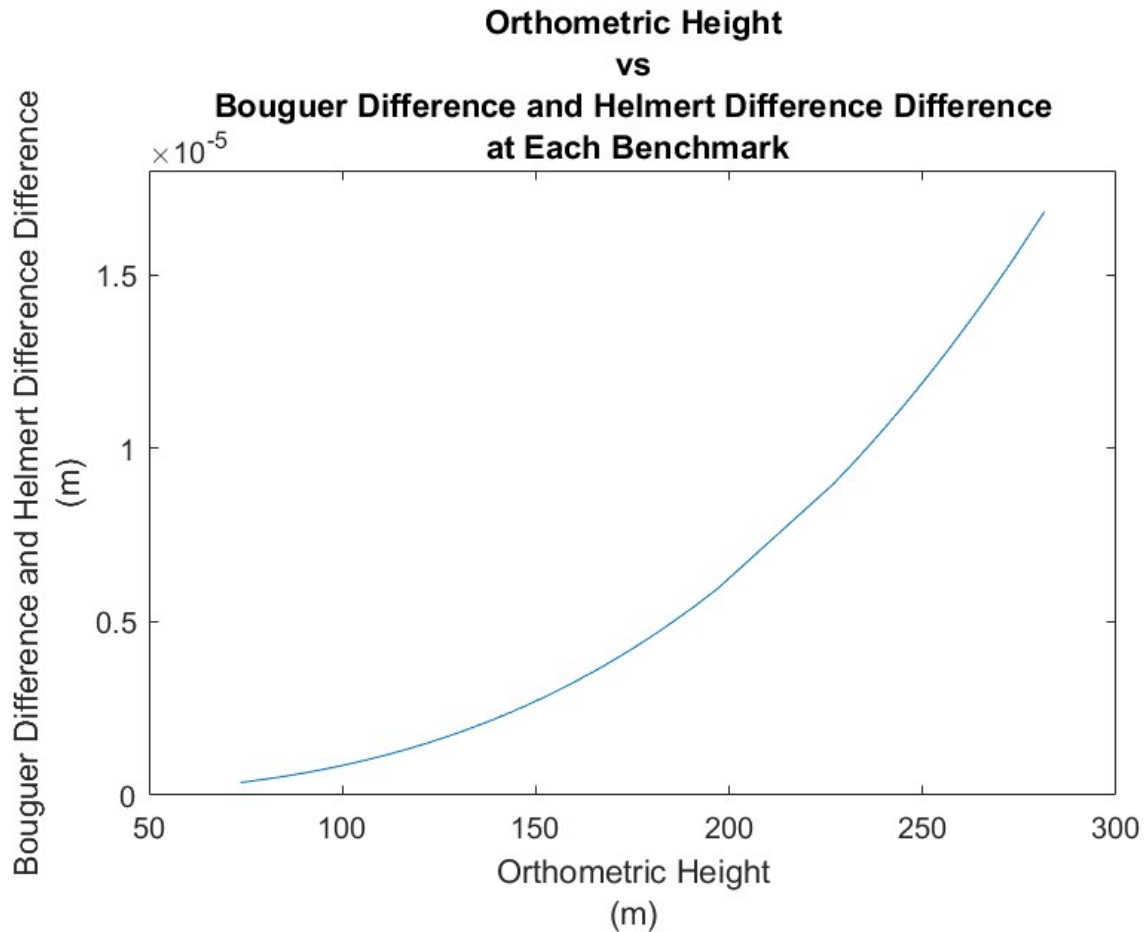


Figure 5: Bouguer Calculated Difference Plotted Against Orthometric Height

Figure 5 shows the calculated difference between orthometric, and normal height plotted against the calculated difference using the Bouguer anomaly. Visual analysis of this figure reveals a potential exponential trend between the two axes. This follows as the Bouguer Anomalies was not as linearly correlated and as the orthometric heights increased, the Bouguer Anomalies stopped increasing, while the actual calculated differences followed a near linear trend and kept increasing as height increased causing a larger difference between the two as orthometric height is increased.

## Task 2

In task 2, the geoid height,  $N$  will be calculated by considering the short, medium and long wavelengths of the geoid. All calculations will be considered for the area defined by: 49°N to 60°N and 118°W to 110°N.

The remove-restore method is applied to find the geoid height by breaking the local geoid into it's frequency contributions into short, medium and long wavelengths. It solves for the geoid height for each

wavelength set by breaking the wavelengths down into three frequencies and then restores all the data by combining them into one final geoid model. [5]

#### Task 2.a) Long Wavelengths

First, the long wavelengths of the geoid height will be determined using the GOCO02S model. [1] This was computed using  $n_{max}=200$ . The model used to calculate this would be defined as: [6]

$$N_{GMGOCO02S} = \frac{GM}{R\bar{\gamma}} \sum_{n=2}^{n_{max}} \left(\frac{R}{r}\right)^{n+1} \sum_{m=0}^n (\delta\bar{c}_{nm} \cos(m\lambda) + \delta\bar{s}_{nm} \sin(m\lambda)) \bar{P}_{nm}(\cos\theta)$$

It uses a spherical harmonic expansion and relies on coefficients that would be provided in the GOCO02S model. This formula would have been applied for all latitudes and longitudes

Based on truncation error, this will reflect in the model having a 54' resolution. To define a better resolution, the medium and shorter wavelengths are required. The data for the model was given and it is visualized below.

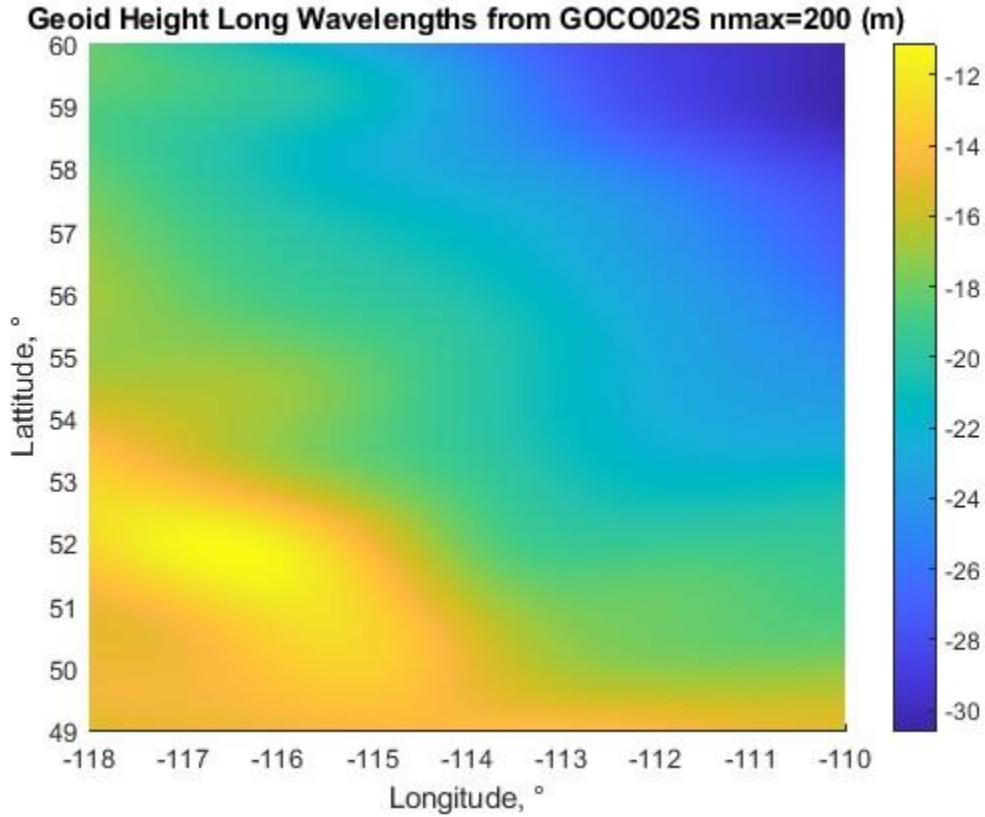


Figure 6: Long Geoid Wavelengths

As can be seen in Figure 6 the long wavelengths present an overall smooth model. There is a negative geoid height in the entire area. There is an increase in the geoid height as it travels from the prairies in the Northeast to the Rocky Mountains in the Southwest.

### Task 2.b) Medium Wavelengths

Next Stokes integral needs to be used to determine medium wavelengths of the geoid height. The Faye anomalies were provided. Using that, the difference between the Faye anomalies and the Geoid height in the long wavelength was determined. This is expressed as: [2]

$$\Delta g = \text{Faye Anomaly} - N_{GOC002S}$$

This was then applied to the Fftgeoid script provided to determine geoid height. It uses Stoke's integral over a 1D plane to apply a fast fourier transform to solve for the geoid height. The solution to Stoke's integral can be expressed as: [6]

$$N_{Stokes} = \frac{G\delta M}{R\gamma} - \frac{\delta W}{\gamma} + \frac{R}{4\pi\gamma} \iint_{\sigma} \Delta g(\psi, \alpha) S(\psi) d\sigma$$

Where  $S(\psi)$  is defined as Stokes kernel and is calculated within the program.

The results of the script is then visualized and displayed below.

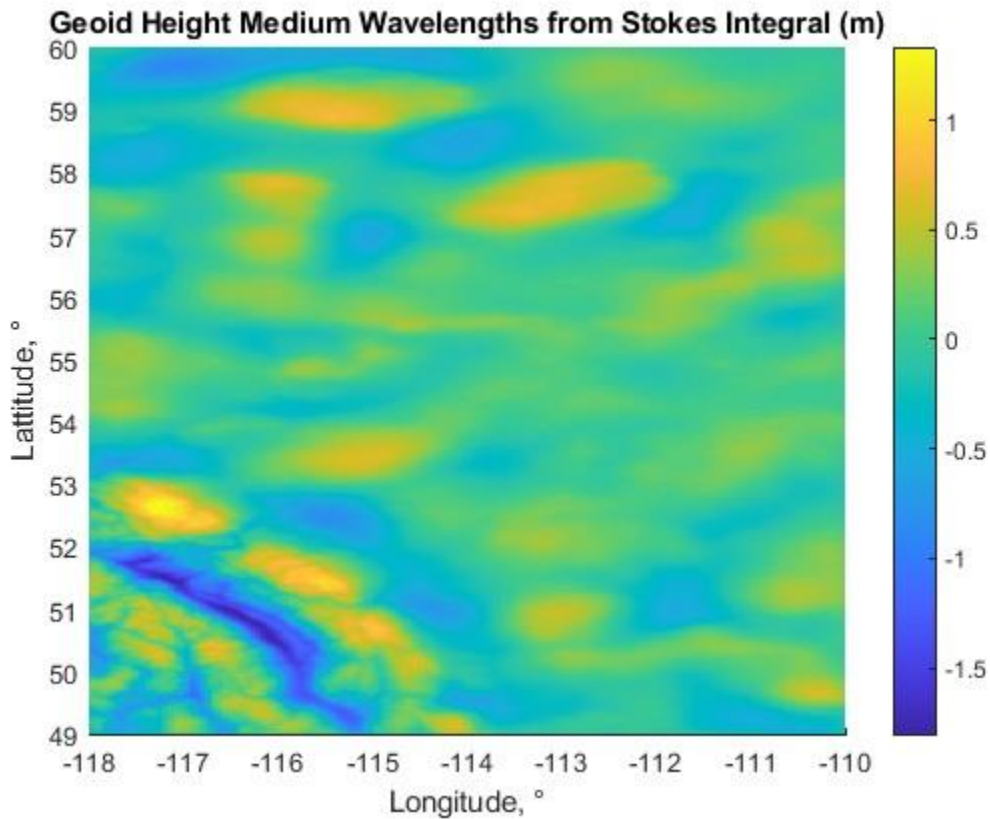


Figure 7: Medium Geoid Wavelengths

Figure 7 demonstrates the medium wavelengths of the geoid height over the study area. The magnitude of the geoid height contribution is significantly smaller than the longer wavelengths with it ranging between approximately -1.5m to 1m instead of -30 to -12m. The medium heights appear to be better distributed around 0m which makes sense as it can be considered a applying a correction surface to the

long wavelengths would should be approximately normally distributed. The medium wavelengths also have a higher resolution with mountain range topography able to be seen slightly more clearly with the specific lines of ranges being clear.

#### Task 2.c) Short Wavelengths

The final wavelengths to be considered are the short wavelengths. These will be determined using an elevation model. The provided script, Ind will then be applied to solve for the geoid height of the short wavelengths. It will perform a terrain reduction to determine the indirect effect using Helmert's condensation reduction by applying a Fast Fourier Transform. It outputs a series of files and the one to be used is indrt.dat that is the summation of the calculated indirect effects. The overall solution can be expressed as: [6]

$$N_{Ind} = -\frac{\pi k \rho}{\gamma} H_P^2 - \frac{G \rho}{6 \gamma} \iint_E \frac{H^3 - H_P^3}{l^3} dx dy$$

The result is shown below.

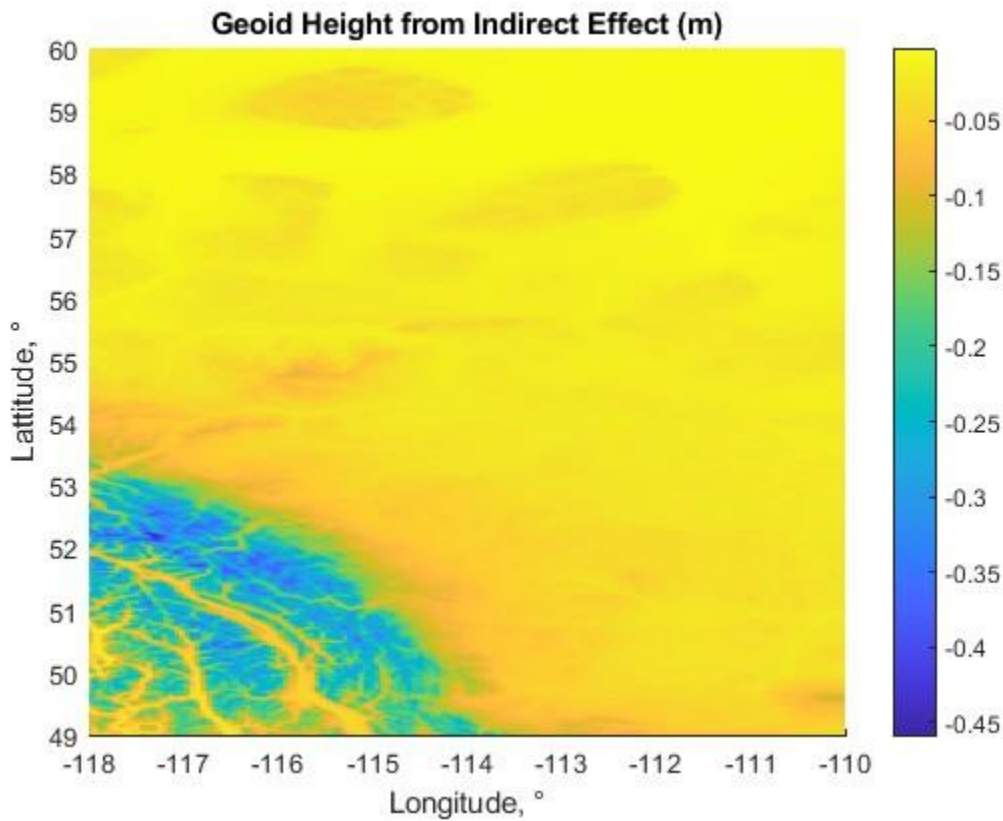


Figure 8: Short Geoid Wavelengths

Figure 8 demonstrates the indirect effect on the geoid height. It has changes of very small magnitudes ranging from -0.05m to -0.45m. Overall, the largest impact on the geoid from the indirect effect can be seen in the Rocky Mountains. This makes sense as it has many changes in elevation and will overall need

more terrain reductions. This model is at a fine resolution that allows that specific mountain ranges and specific mountain to be more clearly seen.

#### Task 2.d) Combined Geoid Height Model

Finally, after solving for the long, medium, and short wavelengths geoid height the overall geoid height needs to be solved for. The overall geoid height was determined by summing the geoid heights at each wavelength range together. [6]

$$N = N_{long\ wavelengths} + N_{medium\ wavelengths} + N_{short\ wavelengths} = N_{GMG002S} + N_{Stokes} + N_{Ind}$$

The combined result is shown below.

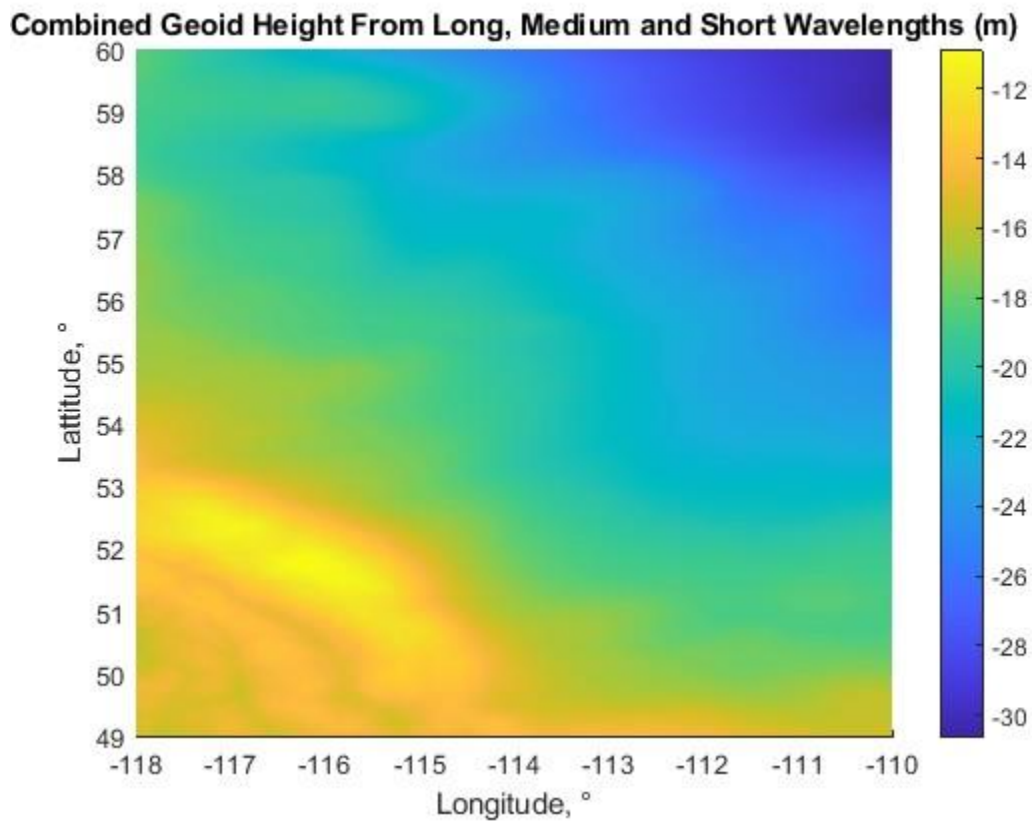


Figure 9: Overall Calculated Geoid Height Model

Figure 9 demonstrates the overall geoid height model. It primarily matches large wavelength model but with a little bit less smooth of a model. The specific variations, especially from the medium wavelength model can be seen in in areas like the mountainous areas where the mountain ranges can be slightly seen unlike in solely the large wavelength model. Overall due to the magnitude of the short wavelengths compared to the long wavelengths the long wavelengths dominate the model leaving the short wavelengths not clearly visible.

#### Task 2.e) EGM2008 Geoid Heights and Summary Statistics

The EGM2008 model with the geoid height was also provided. It was visualized and is shown below. [1]

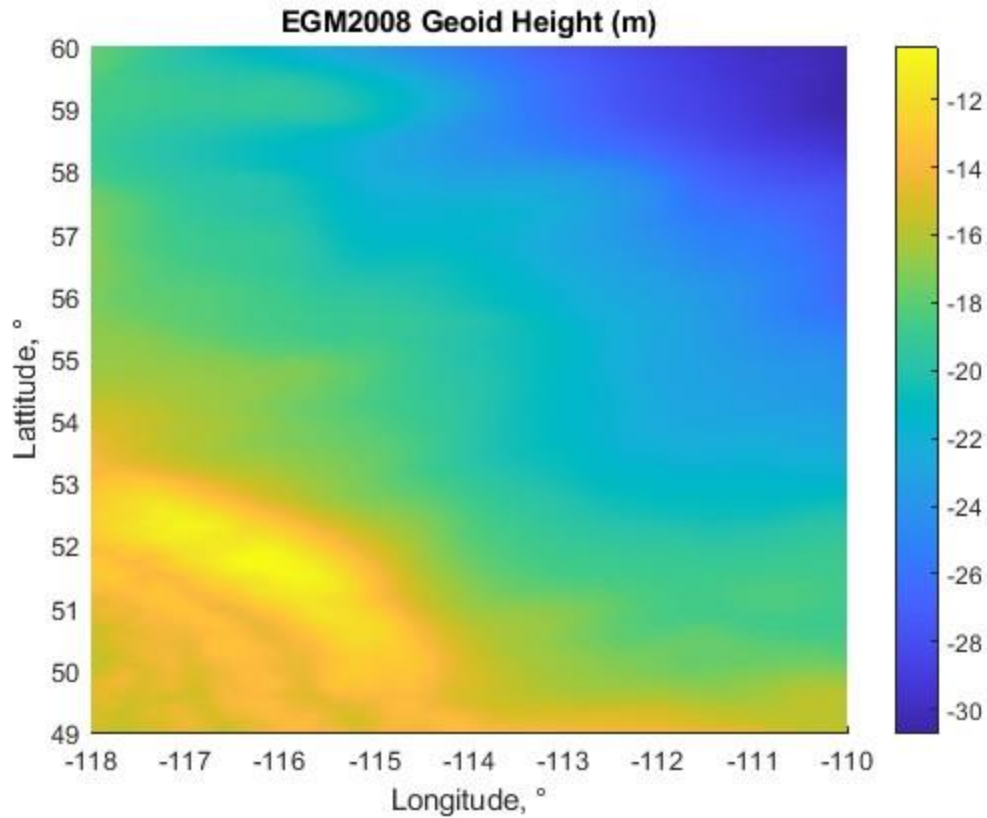


Figure 10: EGM2008 Overall Geoid Height

The above figure appear to be a very close match to the model we generated in this lab. The same details in the geoid height model can be seen. This model and our model also appear to follow the same magnitude of values. To further compare, numerical statistics will be calculated below to see the differences in the models.

Table 6: Statistical Differences Between the Calculated and Final Gravity Model

	N	$N_{EGM2008}$	$N - N_{EGM2008}$
Minimum (m)	-30.598	-30.665	-0.387
Maximum (m)	-10.862	-10.428	0.743
Mean (m)	-19.676	-19.618	0.058
Standard Deviation (m)	4.159	4.260	0.143

Overall N and  $N_{EGM2008}$  display very similar results. They both have a very similar minimum and maximum value which indicates similarity in the dataset. The means across the area are similar at around -16.6m which indicates an overall bias in the geoid height within the area of study.

Looking at the difference between the two models, they are very similar. There is no clear bias between the two models with a mean difference of 0.058m. Additionally the range of differences is very small with only a 0.143m standard deviation. With these statistics it can be determined that our geoid height model as successfully computed and can be considered accurate against the provided model

## Conclusion

Overall, a series of calculations using the normal heights and the gravity values for benchmarks along a levelling line was successfully computed. First, the geopotential numbers were computed and used to find the Helmert/Orthometric height, and the dynamic heights based on the given set of benchmarks. Next, gravity anomalies and Bouguer anomalies were calculated and plotted with respect to Normal Heights and their correlations were discussed. Finally, the Bouguer anomalies were used to calculate an estimated difference between the Orthometric and Normal heights which was compared to the real calculated difference found earlier in Task 1.

The remove-restore method was successfully applied to determine the local geoid height in a section of Canada. The local geoid height was determined and compared against the EGM2008 geoid height. It was found that these were very similar indicating that the local geoid height was successfully solved for. The long wavelengths were solved by spherical expansion, the medium wavelengths by the Stokes integral and the short wavelength by the indirect effect. Overall, this leads to a comprehensive solution that accurately matched a known model.



## References

- [1] M. J. Dehghan, E. Rangelova, "ENGO 423\_W2024\_Lab5\_Handout" March 2024. [Online]. Available: <https://d2l.ucalgary.ca/d2l/le/content/569768/viewContent/6397077/View>. [Accessed April 2024].
- [2] M. J. Dehghan, E. Rangelova, "Lab5-Instructions" March 2024. [Online]. Available: <https://d2l.ucalgary.ca/d2l/le/content/569768/viewContent/6398202/View>. [Accessed April 2024].
- [3] M. G. Sideris, E. Rangelova, "ENGO423\_W2024\_Chapter 4" March 2024. [Online]. Available: <https://d2l.ucalgary.ca/d2l/le/content/569768/viewContent/63457400/View> [Accessed March 2024].
- [4] H. Moritz, "Geodetic Reference System 1980". [Online]. Available: <https://d2l.ucalgary.ca/d2l/le/content/569768/viewContent/6376048/View> [Accessed March 2024].
- [5] M. G. Sideris, E. Rangelova, "ENGO423\_W2024\_Chapter 8" March 2024. [Online]. Available: <https://d2l.ucalgary.ca/d2l/le/content/569768/viewContent/6398161/View> [Accessed April 2024].
- [6] M. J. Dehghan, E. Rangelova, "ENGO 423\_W2024\_Lab4\_Handout" March 2024. [Online]. Available: <https://d2l.ucalgary.ca/d2l/le/content/569768/viewContent/6376046/View>. [Accessed March 2024].



## Appendix A: MATLAB Code

### ENGO423\_Lab5\_Main.m

```
clc
close all

%Following Code is Autogenerated by MATLAB
%% Set up the Import Options and import the data
opts = spreadsheetImportOptions("NumVariables", 5);

% Specify sheet and range
opts.Sheet = "PR-all";
opts.DataRange = "A3:E112";

% Specify column names and types
opts.VariableNames = ["BM", "fidecimalDegree", "lambdadecimalDegree", "NormalHeightH",
"gmGal"];
opts.VariableTypes = ["double", "double", "double", "double", "double"];

% Import the data
tbl = readtable("Normal_Heights_Gravity_Line1.xls", opts, "UseExcel", false);

%% Convert to output type
BM = tbl.BM;
fiDD = tbl.fidecimalDegree;
lambdaDD = tbl.lambdadecimalDegree;
NormalHeightH = tbl.NormalHeightH;
gmGal = tbl.gmGal;

%% Clear temporary variables
clear opts tbl
%From here it is our own code

importfile("Faye_Anomaly.mat");
importfile("GravityAnomaly_GM_200.mat");
[NormalHeightH,I] = sort(NormalHeightH);

%Initializes vectors
ybar = zeros(size(NormalHeightH,1),1);
ybar45 = zeros(size(NormalHeightH,1),1);
C = zeros(size(NormalHeightH,1),1);
g = gmGal*1E-5;
g = g(I,:);
fiDD = fiDD(I,:);
[NormalHeightH,i] = sort(NormalHeightH);

%Finds gravity values
for i = 1:size(NormalHeightH)
    ybar45(i) = NormalGravity(45);
```

```

[ymbar(i),y(i)] = meanNormalGravity(fiDD(i),NormalHeightH(i));

end

%Finds C values
for i = 1:size(NormalHeightH,1)
    C(i,1) = NormalHeightH(i)*ymbar(i);
end

%Initializes vectros
H = zeros(size(NormalHeightH,1),1);
Hd = zeros(size(NormalHeightH,1),1);

%Finds H values
for i = 1:size(NormalHeightH,1)
    H(i) = OrthoHeight(C(i),g(i),NormalHeightH(i));
    Hd(i) = C(i)/ ybar45(i);
end

%Outputs results
Hcorr = PlotHeights(NormalHeightH-H,NormalHeightH,"Normal Heights","Helmert and
Normal Height Difference");

HdCorr = PlotHeights(H-Hd,H,"Helmert Height","Helmert and Dynamic Height
Difference");

%% Task 1.2

%Finds change in gravitys
deltag = g - NormalGravityatH(fiDD,NormalHeightH);
deltagBouger = g*1E5 - NormalGravityatH(fiDD,NormalHeightH)*1E5 -
0.1119.*NormalHeightH;

gravAnomCorr = PlotGrav(deltag,NormalHeightH,"Normal Height","Gravity Anomalies");
gravAnomBougerCorr = PlotGrav(deltagBouger*1E-5,NormalHeightH,"Normal Height","Bouger
Anomalies");

Bdiff = BouguerDiff(deltagBouger*1E-5,H, ybar);

EmpRelationship = PlotHeights(abs(Bdiff-(NormalHeightH-H)),H,"Orthometric
Height","Bouguer Difference and Helmert Difference Difference");

%% Task 2

%Finds the difference between Faye Anomaly and long wavelength model
FayeDiff = Faye_Anomaly-GravityAnomaly_GM_200;
writematrix(FayeDiff,"FayeDiff.txt");

%% Task 1.1 Functions
function [H] = OrthoHeight(C,g,Hstar)

```

```

    while true
        gMean = g*1E5+(0.0424*Hstar);
        H = C/(gMean*1E-5);

        if abs((Hstar-H)/H)<0.0001
            break
        else
            Hstar = H;
        end
    end
end

function [corr] = PlotHeights(Hdiff,H,xaxis,yaxis)
    figure;
    plot(H,Hdiff,"-")
    xPhrase = [xaxis '(m)'];
    yPhrase = [yaxis '(m)'];
    titlePhrase = [xaxis ' vs ' yaxis ' at Each Benchmark'];

    title(titlePhrase);
    xlabel(xPhrase);
    ylabel(yPhrase);

    corr = corrcoef(Hdiff,H);
end

function [corr] = PlotGrav(Hdiff,H,xaxis,yaxis)
    figure;
    plot(H,Hdiff,"-")
    xPhrase = [xaxis '(m)'];
    yPhrase = [yaxis '(m/s^2)'];
    titlePhrase = [xaxis ' vs ' yaxis ' at Each Benchmark'];

    title(titlePhrase);
    xlabel(xPhrase);
    ylabel(yPhrase);

    corr = corrcoef(Hdiff,H);
end

%% Task 1.2 Functions
function [Bdiff] = BouguerDiff(gB,H,gBar)
    Bdiff = gB.*H./gBar;
end

```

## Task2Plotting.m

```
%Imports all data
importfile("GeoidUndulation_GM_200.mat");
importfile("N_EGM2008_2160.mat");

NStokes = importfileTxt('exe files\NStokes.txt', 2, 7921);
NIND = importfileTxt('exe files\NStokes.txt', 2, 7921);

NStokes = reshape(NStokes',240,330)';
NIND = reshape(NIND',240,330)';

%Plots all results
%% 2.a
plotWavelengths(GeoidUndulation_GM_200)

%% 2.b
plotWavelengths(NStokes)

%% 2.c
plotWavelengths(NIND)

%% 2.d
N = GeoidUndulation_GM_200 + NStokes + NIND;
plotWavelengths(N)

%% 2.e
plotWavelengths(N_EGM2008_2160)

%% Output Statistics
[minN,maxN,meanN,sdN] = statisticsN(N);
[minN08,maxN08,meanN08,sdN08] = statisticsN(N);

function plotWavelengths(data,title)
    %Plots the results across each lat, long
    figure;
    hold on;
    imagesc([-118 -110],[49 90],data)
    hold on
    plot(long,lat);
    xlabel(['Longitude, ' char(176)])
    ylabel(['Latitude, ' char(176)])
    xlim([-180 180])
    ylim([-90 90])
    titlePhrase = ['Gravity Anomaly  $\Delta g$  (mGal) for n=' num2str(n) ',m=' num2str(m)
    ']);
    title(titlePhrase)
    colorbar
end
```

### importFile.m

```
function importfile(fileToRead1)
%IMPORTFILE(FILETOREAD1)
% Imports data from the specified file
% FILETOREAD1: file to read

% Auto-generated by MATLAB on 02-Apr-2024 16:16:41

% Import the file
newData1 = load('-mat', fileToRead1);

% Create new variables in the base workspace from those fields.
vars = fieldnames(newData1);
for i = 1:length(vars)
    assignin('base', vars{i}, newData1.(vars{i}));
end
```

### meanNormalGravity.m

```
function [ybar,y] = meanNormalGravity(lat,Hs)
%Finds ybar based on Hs
y = NormalGravity(lat);

sinl = sind(lat).^2;

a = 6378137;
f = 0.00335281068118;
m = 0.00344978600308;

ybar = y .* (1 - (1 + f + m - 2 .* f .* sinl).*Hs./a + (Hs./a).^2);

end
```

### NormalGravity.m

```
function [y] = NormalGravity(lat)
%Finds gravity on ellipsoid, WGS80
ya = 9.7803267715;
k = 0.001931851353;
e2 = 0.00669438002290;

sinl = sind(lat).^2;

y = ya .* (1.+k.*sinl) ./ sqrt(1.- e2 .* sinl);

end
```

### NormalGravityatH.m

```
function [yH] = NormalGravityatH(lat,h)
%Finds gravity at h above ellipsoid
ya = 9.7803267715;
a = 6378137;
f = 0.00335281068118;
m = 0.00344978600308;

y = NormalGravity(lat);
yH = y .* (1-(2./a)*(1+f+m-2.*f.*sind(lat).*sind(lat)).*h+3.*ya.*h.*h./(a.*a));
end
```